China Geology 6 (2023) 208−215

China Geology

Journal homepage: http://chinageology.cgs.cn
https://www.sciencedirect.com/journal/china-geology

Growth behavior and resource potential evaluation of gas hydrate in core fractures in Qilian Mountain permafrost area, Qinghai-Tibet Plateau

Qing-guo Meng[a, b], Chang-ling Liu[a, b,*], Zhen-quan Lu[c,*], Xi-luo Hao[a, b], Cheng-feng Li[a, b], Qing-tao Bu[a, b], Yun-kai Ji[a, b], Jia-xian Wang[a, d]

[a] *Key Laboratory of Gas Hydrate*, *Qingdao Institute of Marine Geology*, *China Geological Survey*, *Ministry of Natural Resources*, *Qingdao* 266237, *China*
[b] *Laboratory for Marine Mineral Resources*, *Laoshan Laboratory*, *Qingdao* 266237, *China*
[c] *Oil and Gas Survey*, *China Geological Survey*, *Ministry of Natural Resources*, *Beijing* 100083, *China*
[d] *Faculty of Engineering*, *China University of Geosciences*, *Wuhan* 430074, *China*

ARTICLE INFO

Article history:
Received 21 July 2022
Received in revised form 13 January 2023
Accepted 24 March 2023
Available online 29 March 2023

Keywords:
Gas hydrate
Growth behavior
Core fracture
Rock Quality Designation
Resource potential evaluation
Engineering
Oil and gas exploration
Qilian Mountain permafrost area
Qinghai-Tibet Plateau

ABSTRACT

The Qilian Mountain permafrost area located in the northern of Qinghai-Tibet Plateau is a favorable place for natural gas hydrate formation and enrichment, due to its well-developed fractures and abundant gas sources. Understanding the formation and distribution of multi-component gas hydrates in fractures is crucial in accurately evaluating the hydrate reservoir resources in this area. The hydrate formation experiments were carried out using the core samples drilled from hydrate-bearing sediments in Qilian Mountain permafrost area and the multi-component gas with similar composition to natural gas hydrates in Qilian Mountain permafrost area. The formation and distribution characteristics of multi-component gas hydrates in core samples were observed *in situ* by X-ray Computed Tomography (X-CT) under high pressure and low temperature conditions. Results show that hydrates are mainly formed and distributed in the fractures with good connectivity. The ratios of volume of hydrates formed in fractures to the volume of fractures are about 96.8% and 60.67% in two different core samples. This indicates that the fracture surface may act as a favorable reaction site for hydrate formation in core samples. Based on the field geological data and the experimental results, it is preliminarily estimated that the inventory of methane stored in the fractured gas hydrate in Qilian Mountain permafrost area is about 8.67×10^{13} m^3, with a resource abundance of 8.67×10^{8} m^3/km^2. This study demonstrates the great resource potential of fractured gas hydrate and also provides a new way to further understand the prospect of natural gas hydrate and other oil and gas resources in Qilian Mountain permafrost area.

1. Introduction

As a new energy resource with great potential, gas hydrate is widely distributed in seabed and permafrost areas. It is estimated that the global inventory of methane stored in hydrate-bearing sediments is as high as 2.1×10^{16} m^3 (Kvenvolden KA, 1988; Milkov AV, 2004). In recent years, gas hydrate researches have been developing rapidly in China's marine and terrestrial permafrost areas (Li JF et al., 2018; Ye JL et al., 2020; Zhu YH et al., 2021; Zhu YH et al., 2010). As one of the main terrestrial permafrost areas in China, Qilian Mountain permafrost area in the Qinghai-Tibet Plateau has broad resource prospects with abundant gas sources and superior formation conditions for gas hydrate (Wang PK et al., 2019). A series of achievements have been made in the exploration and trial production of terrestrial hydrate resources in China, ever since gas hydrate samples were obtained in Qilian Mountain permafrost area for the first time in 2008 (Zhu YH et al., 2021).

The formation of gas hydrate is not only affected by the temperature and pressure conditions, but also closely related to the geological characteristics, fluid properties (gas and water) and the space of occurrence layer. The hydrate-bearing sediments in Qilian Mountains permafrost area are consolidated rocks such as siltstone, oil shale and mudstone.

First author: *E-mail address*: mengqimg@126.com (Qing-guo Meng).

* Corresponding author: *E-mail address*: qdliuchangling@163.com (Chang-ling Liu); luzhq@vip.sina.com (Zhen-quan Lu).

Literary editor: Xi-jie Chen
doi:10.31035/cg2023021
2096-5192/© 2023 China Geology Editorial Office.

The area has well-developed fractures which obviously control the distribution of hydrate (Wang PK et al., 2011). Gas hydrates in this area contain high contents of heavy hydrocarbon molecules (C_2H_6, C_3H_8 and C_4H_{10}) and small non-hydrocarbon molecules (CO_2 and H_2S; He XL et al., 2015; Huang X et al., 2011; Liu CL et al., 2015; Meng QG et al., 2015). The gas components and occurrence characteristics of gas hydrates in Qilian Mountain permafrost area are significantly different from those of marine gas hydrates (He XL et al., 2015; Zhu YH et al., 2021). Laboratory experiments have been conducted to study the special occurrence characteristics of hydrates in this area (Meng QG, 2019; Meng QG et al., 2022). Li CF et al. (2015) confirmed that the core samples in this area have well-developed fractures with good connectivity by X-ray Computed Tomography (X-CT). Su K et al. (2016) studied the formation characteristics of methane hydrate in fractured core from Qilian Mountain permafrost area, and the influencing factors on the formation process of multi-component gas hydrate in pure water was studied by Tian M (2018). Meng QG et al. (2022) compared the growth behavior of multi-component hydrate in pure water, mine water and permafrost cores. They found that the multi-component gas hydrates formed more quickly in the permafrost core media (mine water and fractured cores) cores than in pure water, meanwhile, the formation process showed a significant "interface priority" phenomenon. It shows that the multi-component gas hydrate has great potential for rapid formation and accumulation in the fractured rocks. Therefore, it is worthwhile to further study the growth behavior and resource potential of multi-component gas hydrates in Qilian Mountain permafrost area.

Volumetric estimation method is commonly used to estimate gas hydrate resources. The basic assumption of this method is that hydrates are continuously distributed in the reservoir both in vertical and horizontal directions. Then the total hydrate resource can be calculated according to following equation:

$$Q = S \times H \times K \times B \times E \quad (1)$$

where Q is the total gas resource of gas hydrate under the standard conditions in the assessment area (m^3), S is the area of hydrate bearing layer (m^2), H is the thickness of hydrate bearing layer (m), K is the porosity of hydrate bearing layer (%), B is the saturation of gas hydrate (%), E is the volume number of gas stored in 1 vol of gas hydrate at standard temperature and pressure condition (Lu ZQ et al., 2010b). Obviously, accurate acquisition of the area, thickness, porosity and saturation of gas hydrate reservoir is essential for precise estimation of the hydrate resources by this method. Besides, Lu ZQ et al. (2007) proposed a new gas hydrate resources calculation method by integration. This method also assumes that the gas hydrates in the reservoir are evenly distributed. However, gas hydrates are often unevenly distributed. Only based on targeted experimental data can the accuracy of gas hydrate resource estimation be increased. Therefore, we creatively combined the experimental simulation with the field observation, and proposed a new method to evaluate the resources of fractured hydrate in the Qilian Mountain permafrost area. Firstly, the geological background of the Qilian Mountain permafrost area was analyzed, and then the formation behavior and distribution characteristics of multi-component gas hydrate in cores from the hydrate accumulation zone were studied using *in situ* X-CT. Finally, combined with field geological data, the resource of gas hydrate in Qilian Mountain permafrost area was estimated.

2. Geological background

The area of Qilian Mountain permafrost area is about 10×10^4 km^2, with the altitude between 3500–4100 m. The lower boundary of the permafrost area on the south slope of Qilian Mountain is about 3700–3900 m above sea level, mainly distributed along the Laji Mountain-Qinghai Nanshan-Qaidam Mountain. The lower boundary of the permafrost area on the north slope is 3450–3650 m, mainly distributed along the Lenglongling-corridor Nanshan-Danghe Nanshan. The lower boundary of the permafrost area has an annual average temperature of −2–2.5°C (Zhou YW et al., 2000). The annual average surface temperature in the permafrost area is 0–2.4°C and the thickness of the frozen soil is 8.0–139.3 m. The permafrost area can be divided into continuous permafrost area and island-like permafrost area. The continuous permafrost area is mainly distributed in the middle of Qilian Mountain. The annual average surface temperature of this area is −1.5–2.4°C and the thickness of frozen soil is 50.0–139.3 m. The island-like permafrost area is distributed in the east and west part of Qilian Mountain. The annual average surface temperature of this area is 0–1.5°C, and the thickness of frozen soil ranges from a few meters to tens of meters(Zhou YW et al., 2000).

In 2008 and 2009, China Geological Survey carried out a series of drilling work in Qilian Mountain permafrost area, and obtained natural gas hydrate samples (Zhu YH et al., 2010). The gas hydrate samples are white or grayish white in color, which can be ignited. Various phenomena referring gas hydrate samples include: bubbling and water seepage on the sample surface, high-pressure gas in the borehole, heavy hydrocarbon spots and residual fine honeycomb structure after the core is dried, authigenic calcite with intact crystal, thermal infrared low-temperature anomaly, etc. (Lu ZQ et al., 2010a). The characteristic peak of hydrocarbon gas of gas hydrate can be identified while processing laser Raman spectrum analysis (Meng QG et al., 2011; Zhu YH et al., 2010). The geophysical logging curves showed obvious high resistivity and high acoustic velocity signals for the core section containing gas hydrates (Lu ZQ et al., 2010b).

Drilling work revealed that gas hydrates are mainly formed in pores or fractures of sandstone and fractures of mudstone, oil shale, siltstone which is 130–400 m below the frozen soil layer (see Table 1). The visible gas hydrates are mainly distributed in the fractures.

Table 1. Characteristics of gas hydrate in Qilian Mountain permafrost area (Lu ZQ et al., 2010b).

Borehole No.	Section/m	Hydrate occurrence	Lithology	Depth of borehole/m
DK1	133.5–135.5	Pores and fractures	Grey-white grey fine sandstone, mainly quartz and kaolinized feldspar	182.23
	142.9–147.7	Fractures	Grey-dark grey siltstone and mudstone, fracture developed	
	165.3–165.5	Pores and fractures	Grey-dark grey pelitic siltstone, fracture developed	
	169.0–170.5	Pores and fractures	Grey-dark grey siltstone, fracture developed	
DK2	144.4–152.0	Pores and fractures	Light grey-taupe mid-fine grained sandstone，mainly quartz and feldspar，fracture developed	635.20
	156.3–156.6	Fractures	Taupe oil shale, fracture developed, 6–8 lines/cm， 0.5–1.0 mm in-width	
	235.0–291.3	Fractures	Brown-dark grey shale and oil shale, fracture developed	
	377.3–387.5	Pores	Grey-grey white mid grained sandstone, mainly quartz and feldspar, contain large amounts of charcoal, fracture developed	
DK3	133.0–156.0	Fractures	Grey brown-black brown mudstone, oil shale, fractures well-developed	765.01
	225.1–240.0	Fractures	Grey-dark grey mudstone, oil shale, fracture developed	
	367.7–396.0	pores and fractures	Grey white-grey brown siltstone, mainly quartz and feldspar, contain small amounts of charcoal, fracture developed	

3. Samples and methods

3.1. Experimental devices

The schematic diagram of the self-designed X-ray CT scanning apparatus for gas hydrate is show in Fig. 1. The core sample is hold by a cylindrical vessel with an inner diameter of 10 mm and an inner height of 60 mm. The cylindrical vessel is made of aluminum alloy and fixed on a rotating platform. The maximum operating pressure of cylindrical vessel is 15 MPa. The gas pressure is measured by a pressure transducer with a precision of ±0.1 MPa. The cylindrical vessel and its inside specimen are cooled down together by a semiconductor cooling system. A resistance thermometer sensor (Pt100) with a precision of ±0.1°C is used to measure the temperature. The experimental apparatus has been described in detail in the previous literatures (Hu GW et al., 2014; Li CF et al., 2013; Li CF et al., 2016; Li CF et al., 2019).

3.2. Samples

The experimental materials in this study mainly include deionized water, multi-component gas, NaCl solution and core samples from hydrate reservoir in Qilian Mountain permafrost area.

The multi-component gas used to study the distribution of the multi-component gas hydrate was artificially prepared based on the composition of dissociated gas of hydrate from Qilian Mountain permafrost area(He XL et al., 2015; Liu CL et al., 2015). The compositions of multi-component gas and the volume ratio of each composition are shown in Table 2.

The two core samples used in this study were both from DK2 borehole in the hydrate discovery region of the Qilian Mountain permafrost area, with burial depths of 142 m and 226.8 m respectively. The core samples were cut into cylinders about 15 mm in high and 9.5 mm in diameter so that they could be put into the cylindrical vessel.

NaCl solution is often used to replace pure water in practice to improve the gray scale difference between hydrate and solution in CT images (Jin S et al., 2004; Li CF et al., 2013). In this study, NaCl solution with 4.0% mass concentration was used to form gas hydrate in the core samples in order to enhance the recognition effect of CT images.

3.3. Experimental procedure and analytical method

The experiments of multi-component hydrate formation were completed based on the self-designed X-ray CT scanning apparatus for gas hydrate shown in Fig. 1. In order to relatively truly simulate the growth behavior and distribution state of hydrate in frozen soil cores, the core samples used in the experiment were carefully cleaned with deionized water and dried at 100°C for 24 h. While removing the fine particles and residual water on the core surface during grinding process, the changes of core fractures were avoided as far as possible. Secondly, the dried core samples were loaded into the cylindrical vessel, and an appropriate amount of 4.0% NaCl solution was added. The cylindrical vessel was fixed on the detection platform of the X-CT scanner after its upper cap was tightened. Thirdly, the cylindrical vessel was connected the gas supply line as shown in Fig. 1, and air in the cylindrical vessel was removed by conducting the multi-component gas injection and release for three times. The multi-component gas flowed into the vessel through the check valve and gas pipe when the cylinder valve was opened. In order to avoid the influences of rapid gas injection on the distribution of water in the cores, the injection of gas into the cylindrical vessel was carefully controlled by the needle valve. The multi-component gas was kept injecting into the cylindrical vessel until the inner pressure reached the target value. Finally, when the gas was fully dissolved in the NaCl solution and the pressure in the vessel was stable, the temperature of the cylindrical vessel was reduced to 275K by adjusting the temperature controller of the semiconductor cooling system. The hydrate formation experiment began at this moment. Hydrate formation was considered complete when the gas pressure decreased and remained unchanged for at least 6 hours. Table 3 shows the experimental working conditions of hydrate formation in core fractures.

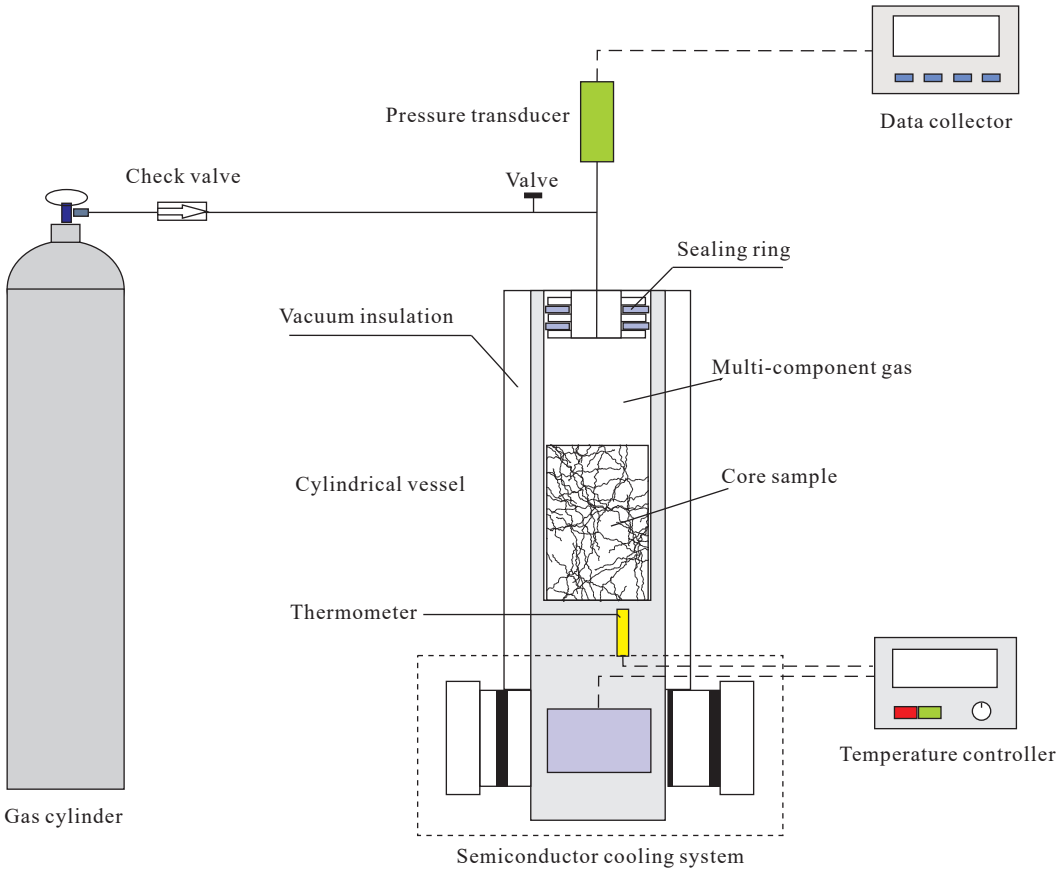

Fig. 1. Schematic diagram of the experimental device.

Table 2. Compositions of multi-component gas sample in the experiments.

Components	C1	C2	C3	*i*-C4	*n*-C4	*n*-C5	CO_2
Volume ratio/%	76.75	10.90	7.44	0.76	2.22	0.85	1.08

Table 3. The experimental working conditions of hydrate formation in core fractures.

No.	Cores	Initial pressure/MPa	Termination pressure/MPa	Temperature/K
1	DK2-142 m	2.2	1.7	275
2	DK2-266.8 m	2.3	1.86	

A high-resolution X-CT scanner (Phoenix X-ray v|tome|xs, GE Sensing & Inspection Technologies) was applied to perform *in situ* scans during hydrate formation and dissociation in core samples. Series of X-CT raw slices of different reaction stages were obtained. During X-CT scan processes, the working parameters X-ray source was: 100 kV as voltage and 80 μA as current, and the detector exposure time is 333 ms. The voxel resolution in reconstructed digital cores was about 16 μm. Due to the high contrast among the different phases in the cylindrical vessel, phase segmentation was conducted by using an optimized Feldkamp algorithm in VG Studio MAX (Volume Graphics). Based on the reconstructed X-CT images, hydrate saturation and phase distribution characteristics were determined in different reaction stages. When processing micro-CT reconstructed images, we also used an edge detection algorithm based on gradient amplitude images to help identify the spatial boundaries between hydrates and other components. For a detailed introduction to the method, please refer to (Zhang W et al., 2016).

4. Results and discussions

4.1. Growth behaviors of multi-component gas hydrates in core fractures

X-CT images obtained during the growth and dissociation of hydrates at the same cross section in the core sample (DK2-142 m) is shown in Fig. 2. There is an obvious fracture on the cross section of the core sample (DK2-142 m), as shown in Fig. 2a. After the injection of NaCl solution, the fracture is full-filled with the NaCl solution, as shown in Fig. 2b. This demonstrates that the fracture has good connectivity. Owing to the good contact between multi-component gas and water, gas hydrates are mainly distributed in the fracture or surrounding the core sample after the hydrate formation, as shown in Fig. 2c. On the contrary, the hydrate formation in the pore space would probably constrain the migration of local fluids. It subsequently hinders the formation of gas hydrate in the closed or partial closed fractures. Based on the CT image analysis, hydrate saturation (ratio of hydrate volume to fracture volume) was calculated to be around 96.8% in factures after the hydrate formation. X-CT images obtained in the process of hydrate dissociation in the core sample are shown in Fig. 2d–2f. In the process of gradient

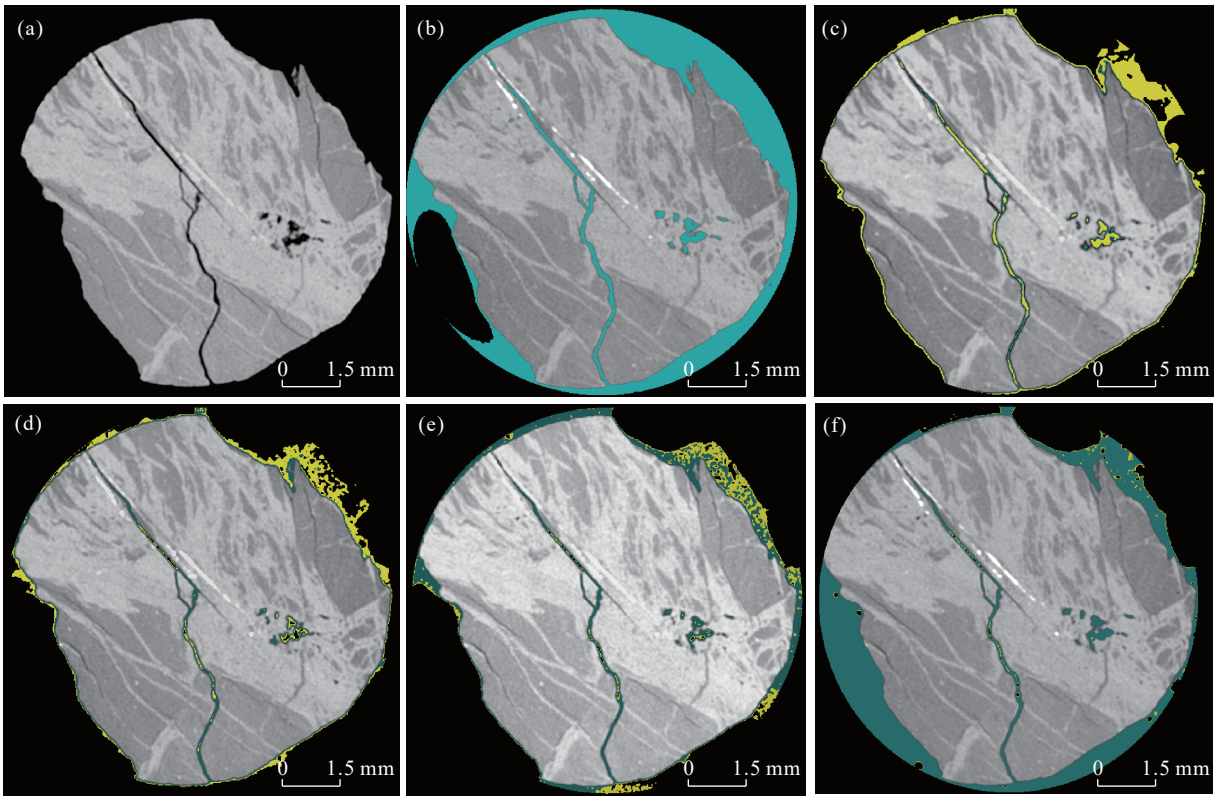

Fig. 2. X-CT images showing the changes during the growth and dissociation of hydrates at the same cross section in core sample DK2-142 m. a–dry sample; b–wet sample; c–f–hydrate-bearing samples with hydrate saturation 96.8%; 42.9%; 24.3% and 5.3%, respectively. (mixed gas; hydrate; water; rock)

heating, gas hydrates located both at sample surface and in the fractures are synchronously dissociated. This indicates that the good fracture connectivity is beneficial to the diffusion and migration of fluid phases during the hydrate formation/dissociation.

The X-CT image of the vertical section of another core sample (DK2-266.8 m) is shown in Fig. 3. Compared with the core sample (DK2-142 m), the fractures in this core sample are of different sizes and irregular distribution. The magnification of the rectangular box in Fig. 3 is shown in Fig. 4. The phase distribution in the fracture before and after hydrate formation are shown in Fig. 4b and Fig. 4c, respectively. Because of the excellent connectivity of the fractures, it is quite easy for fluid phases to penetrate the core sample. Moreover, free water entered the fractures is mostly distributed along the pore surface because of the good hydrophilicity of the rock. During the formation of hydrate, water on the pore surface is gradually consumed while hydrate forms along the gas-liquid interface and gradually expand to the whole fracture space. With the complete consumption of water in the fracture, multi-component gas phase could retain in the fracture space. Based on the X-CT image analysis, the hydrate saturation was calculated to be around 60.67% in factures after the hydrate formation.

Based on the above experimental results, it can be concluded that the core samples in Qilian Mountain permafrost area are rich in fractures with good connectivity. The growth and distribution of multi-component gas hydrate

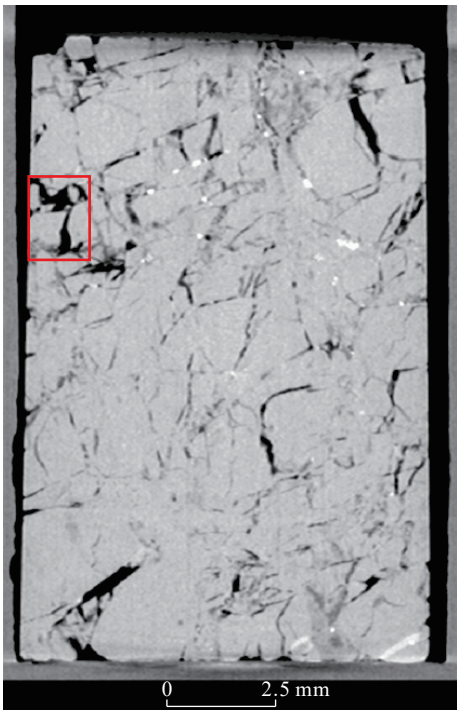

Fig. 3. The vertical profile of the core sample DK2-266.8 m. The magnification area of the red rectangle is shown in Fig. 4.

showed obvious "interface advantage". Fractures not only provide storage space for multi-component gas hydrate, but also provide favorable conditions for hydrate formation and accumulation. The above understanding is of great

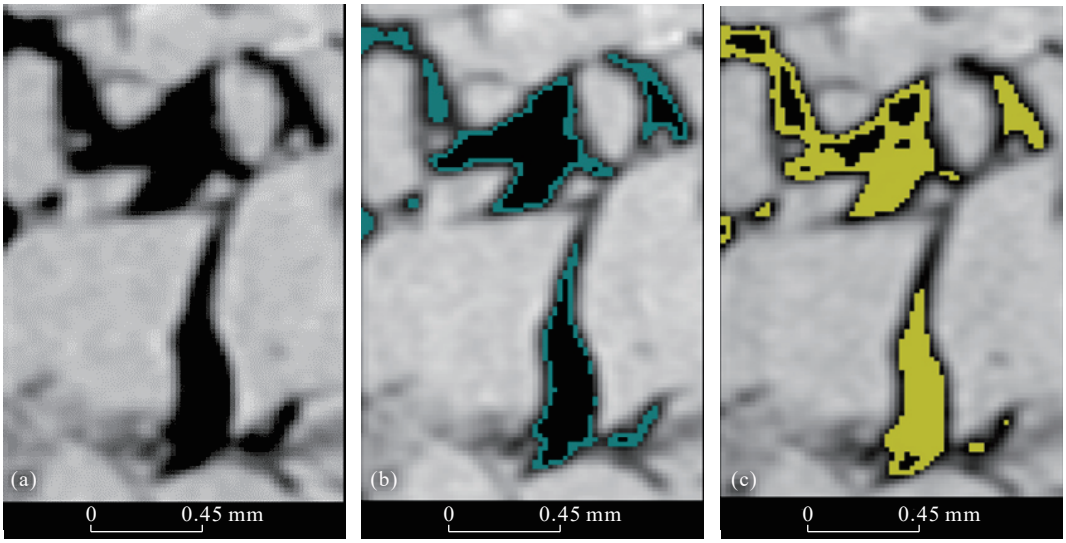

Fig. 4. Hydrate growth in local fractures in core sample DK2-266.8m. a–dry sample; b–wet sample; c–hydrate-bearing sample with hydrate saturation 60.67%. (gas; hydrate; water; rock)

significance in understanding the accumulation mechanism of natural gas hydrate and accurately evaluating the hydrate reservoir resources in Qilian Mountain.

4.2. Resource potential evaluation of gas hydrate

Drilling has shown that gas hydrates mainly occurred in rock fractures in Qilian Mountain permafrost area which is the main focus of resources evaluation in this study.

For resources potential evaluation of gas hydrates, one should first consider the thickness of rock layer in the stability zone of gas hydrates. However, gas hydrate in this area is only filled in the fractures of rock. Thus, the gas hydrates distributed in the reservoir can be calculated by the following equation (Lu ZQ et al., 2010b):

$$Q_1 = A \times \lambda \times H \times F_1 \times F_2 \times L \times S_1 \times E \quad (2)$$

where Q_1 is the gas hydrate resource in the evaluation area; A is the distribution area of gas hydrate which is 10×10^4 km^2; λ is the probability of occurrence of gas hydrate on the plane which is 0.75 as indicated by the drilling data; H is the thickness of the gas hydrate stability zone which starts from 130 m to 400 m as indicated by the drilling data which is 270 m; F_1 and F_2 are the fragmentation degree and fracture density of the rock in gas hydrate stability zone, respectively; L is the width of each fracture; S_1 is hydrate saturation in the fracture which is 78.74 % based on the arithmetic average of the experimental data; E is the volume number of gas stored in 1 vol of gas at standard P-T condition which is 160.

Rock Quality Designation (RQD) is a statistical index of rock integrity in the process of core logging, and the degree of fragmentation can be obtained through rock integrity statistics (Zhang L, 2016). In the process of compiling permafrost hydrate cores, the RQD values of the borehole DK2 and DK3 is calculated by using the stage statistical method combined with lithologic stratification. This is to calculate the percentage of the length of columnar core greater than 10 cm in each lithologic stratification to the thickness of that stratification. It is found that the low RQD values stage of the borehole DK2 and DK3 is in good agreement with the hydrate reservoir sections, which indicates that gas hydrate tends to be stored in the fracture-development section (Wang PK et al., 2011). In borehole DK2, RQD values of 18 layers in gas hydrate stability zone were counted with an average value of 31.68%. Based on this calculation, the average fragmentation degree in the gas hydrate stability zone for borehole DK2 is 68.32%. Meanwhile, RQD values of 7 layers in the gas hydrate stability zone were counted with an average of 36.46%, and the average fragmentation degree for borehole DK-3 is 63.54%. Therefore, boreholes DK2 and DK3 have similar fragmentation degree and RQD values. In this study, we use the average RQD value (34.07%) for resources evaluation, thus the fragmentation degree (F_1) used in resources evaluation is 65.93% (Lu ZQ et al., 2010b).

The parameters used in gas hydrate resource evaluation are summarized in Table 4. Based on these parameters and Eq. 2, the total gas hydrate resource (Q_1) in fractures of this area was calculated to be equal with 8.67×10^{13} m^3 methane.

The essence of gas hydrate resources evaluation is to estimate the amount of effective natural gas that can be released during hydrate dissociation (Sun YB et al., 2013). Currently, there is no systematic and standard resources evaluation method for gas hydrate. Therefore, the gas hydrate resources in this area were classified based on the National Standard GB/T 19492-2004 “Classifications for petroleum resources/reserves”. Since the exploitation of gas hydrate has not yet entered the stage of commercial exploitation, the classification of recoverable amounts, reserve status and

Table 4. Parameters used in hydrate resource evaluation in Qilian Mountain permafrost area.

Parameters	Values in evaluation	Parameters	Values in evaluation
A /m^2	10×10^{10}	F_1 /%	65.93
λ	0.75	F_2 /lines per m	68.7
H /m	270	L /m per line	7.5×10^{-4}
E	160	S_1 /%	78.74

economic significance are not considered in current classification of gas hydrate resources. From the perspective of geological control degree, the natural gas hydrate resources are divided into total resources in place, geological reserves and undiscovered total resources in place. The geological reserves include measured, indicated and inferred reserves in place, and the undiscovered total resources in place include potential and predicted resources in place. The estimated amount of hydrate resources in this study refers to the total resources in place. Accordingly, the methane gas resource abundance of the total gas hydrate in Qilian Mountains permafrost area is 8.67×10^8 m^3/km^2.

According to the classification standards of natural gas fields (shown in Table 5), gas hydrate resources in Qilian Mountains permafrost area are equivalent to shallow, medium abundance and large gas field. The hydrate resource abundance in the Qilian Mountain permafrost area is basically consistent with the resource abundance of nine hydrate enrichment zones worldwide, which is about 2×10^9–14×10^9 m^3/km^2 (Wang F and Li HJ, 2010). From the perspective of resource development and utilization, the total gas reserves will become an important consideration for the sustainable development of gas hydrate resources in this area. From the perspective of production technology, commercial exploitation of gas hydrate is far from perfect. The occurrence of gas hydrate in this area is volatile and influenced by a variety of factors, which would also hinder the effective development of the hydrate resources (Li YH et al., 2015). Based on current understanding on geological background, hydrate resources and exploitation technology of gas hydrate in Qilian Mountains permafrost area, the primary task is to further investigate and clarify the natural gas hydrate resources in this region.

5. Conclusions

In this study, *in situ* X-ray CT scans on the formation and dissociation process of multi-component gas hydrate in fractured cores from Qilian Mountain permafrost area of the Qinghai-Tibet Plateau were performed, and the growth behavior and distribution characteristics of the gas hydrate were studied. Based on the experimental results and the field geological data of gas hydrate reservoir in Qilian Mountain permafrost area, the potential abundant of hydrate resources in this area was preliminarily evaluated. The main conclusions are as follows:

(i) Fractures are well developed in the core samples collected from the Qilian Mountains permafrost area. Multi-component gas hydrate is mainly distributed in the core fractures with good connectivity. The saturations of hydrate in fractures are 96.8% and 60.67% for the two core samples, respectively, with an average value of about 78.74%. The development of core fractures provides favorable space for the massive occurrence of hydrate.

(ii) The total gas hydrate resources in the drilling area (10×10^4 km^2) are estimated to be equal to 8.67×10^{13} m^3 methane, with a resource abundance of 8.67×10^8 m^3/km^2, which is basically consistent with the enrichment zones of gas hydrate worldwide. Hydrate growth behavior is actually affected by the local environment. The evaluation of hydrate resources based on experiments is related to the final production of the fractured hydrate in the experiment. However, it still provides a new way to further understand the resource potential of gas hydrate and other oil and gas resources in Qilian Mountain permafrost area, the Qinghai-Tibet Plateau.

CRediT authorship contribution statement

Qing-guo Meng, Chang-ling Liu and Zhen-quan Lu conceived of the presented idea. Chang-ling Liu and Zhen-quan Lu supervised the findings of this work and were in charge of overall direction and planning. Qing-guo Meng and Cheng-feng Li carried out the experiment. Qing-guo Meng, Xi-luo Hao, Cheng-feng Li, Qing-tao Bu, Yun-kai Ji and Jia-xian Wang contributed to the interpretation of the results. All authors provided critical feedback and contributed to the final manuscript.

Declaration of competing interest

The authors declare no conflicts of interest.

Acknowledgements

The authors greatly appreciate the financial support of the National Natural Science Foundation of China (42176212, 41976074 and 41302034), the Marine S&T Fund of Shandong Province for Laoshan Laboratory (2021QNLM020002) and the Marine Geological Survey Program (DD20221704). The authors would like to extend their sincere gratitude to the reviewers and editors for their responsible and valuable comments on this manuscript.

Table 5. Classification standards of natural gas field scales.

Classification	High production	Medium production	Low production	
Stable natural gas production of a single well with a depth of 1000 meters/10^4 m^3/(km.d)	>10	3–10	<3	
	High abundance	Medium abundance	Low abundance	
Reserves abundance of natural gas fields/10^8 m^3/km^2	>10	2–10	<2	
	Large gas fields	Medium gas fields	Small gas fields	
Total reserves of natural gas fields/10^8 m^3	>300	50–300	<50	
	Shallow layer	Medium-deep layer	Deep layer	Ultra-deep layer
Buried depth of natural gas reservoir (field)/m	<1500	1500–3200	3200–4000	>4000

References

He XL, Liu CL, Meng QG, Lu ZQ, Wen HJ, Li YH, Zhang SL, Wang JT. 2015. Gas composition of hydrate-bearing cores in Juhugeng drilling area in Qinghai and its indicative significance. Geoscience, 29(5), 1194–1200 (in Chinese with English abstract). doi: 10.3969/j.issn.1000-8527.2015.05.024.

Hu GW, Li CF, Ye YG, Liu CL, Zhang J, Diao SB. 2014. Observation of gas hydrate distribution in sediment pore space. Chinese Journal of Geophysics, 57(5), 1675–1682 (in Chinese with English abstract). doi: 10.6038/cjg20140530.

Huang X, Zhu YH, Wang PK, Guo XW. 2011. Hydrocarbon gas composition and origin of core gas from the gas hydrate reservoir in Qilian Mountain permafrost. Geological Bulletin of China, 30(12), 1851–1856 (in Chinese with English abstract). doi: 10.3969/j.issn.1671-2552.2011.12.006.

Jin S, Takeya S, Hayashi J, Nagao J, Kamata Y, Ebinuma T, Narita H. 2004. Structure analyses of artificial methane hydrate sediments by microfocus X-ray Computed Tomography. Japanese Journal of Applied Physics, 43(8A), 5673–5675. doi: 10.1143/jjap.43.5673.

Kvenvolden KA. 1988. Methane hydrate - A major reservoir of carbon in the shallow geosphere? Chemical Geology, 71(13), 4151. doi: 10.1016/0009-2541(88)90104-0.

Li CF, Hu GW, Ye YG, Liu CL, Cheng J, Zhang LK, Zheng RE. 2013. Microscopic distribution of gas hydrate in sediment determined by X-ray computerized tomography. Journal of Optoelectronics · Laser, 24(3), 551–557 (in Chinese with English abstract).

Li CF, Hu GW, Zhang W, Ye YG, Liu CL, Li Q, Sun JY. 2016. Influence of foraminifera on formation and occurrence characteristics of natural gas hydrates in fine-grained sediments from Shenhu area, South China Sea. Science China (Earth Sciences), 59(11), 2223–2230. doi: 10.1007/s11430-016-5005-3.

Li CF, Liu CL, Hu GW, Sun JY, Hao XL, Liu LL, Meng QG. 2019. Investigation on the Multiparameter of Hydrate-Bearing Sands Using Nano-Focus X-Ray Computed Tomography. Journal of Geophysical Research-Solid Earth, 124(3), 2286–2296. doi: 10.1029/2018jb015849.

Li CF, Liu CL, Meng QG, Hu GW, Zhang W, Lu ZQ, Wen HJ, Li YH, Wang WC. 2015. CT image characterization of pores and fissures in rock core from Juhugeng gas hydrate area in Qinghai. Geoscience, 29(5), 1189–1193 (in Chinese with English abstract). doi: 10.3969/j.issn.1000-8527.2015.05.023.

Li JF, Ye J, Qin X, Qiu H, Wu N, Lu H, Xie W, Lu J, Peng F, Xu Z, Lu C, Kuang Z, Wei J, Liang Q, Lu H, Kou B. 2018. The first offshore natural gas hydrate production test in South China Sea. China Geology, 1(1), 5–16. doi: 10.31035/cg2018003.

Li YH, Wang WC, Lu ZQ, Chen X, Fan HJ. 2015. Preliminary evaluation on gas hydrate resources in Sanlutian of Muli, Qinghai. Geoscience, (5), 1251–1258 (in Chinese with English abstract). doi: 10.3969/j.issn.1000-8527.2015.05.030.

Liu CL, Meng QG, He XL, Li CF, Ye YG, Lu ZQ, Zhu YH, Li YH, Liang JQ. 2015. Comparison of the characteristics for natural gas hydrate recovered from marine and terrestrial areas in China. Journal of Geochemical Exploration, 152, 67–74. doi: 10.1016/j.gexplo.2015.02.002.

Lu ZQ, Wu BH, Jin CS. 2007. A method for gas hydrate resource estimation—an example of preliminary estimation of gas hydrates in the northern continental slope, South China Sea. Petroleum Geology & Experiment, 29(3), 319–323 (in Chinese with English abstract). doi: 10.3969/j.issn.1001-6112.2007.03.019.

Lu ZQ, Zhu YH, Zhang YQ, Wen HJ, Li YH, Jia ZY, Liu CL, Wang PK, Li QH. 2010a. Basic geological characteristics of gas hydrates in Qilian Mountain permafrost area, Qinghai Province. Mineral Deposits, 29(1), 182–191 (in Chinese with English abstract). doi: 10.3969/j.issn.0258-7106.2010.01.017.

Lu ZQ, Zhu YH, Zhang YQ, Wen HJ, Li YH, Wang PK. 2010b. Estimation method of gas hydrate resource in the Qilian Mountain permafrost area, Qinghai, China —a case of the drilling area. Geological Bulletin of China, 29(9), 1310–1318 (in Chinese with English abstract). doi: 10.3969/j.issn.1671-2552.2010.09.007.

Meng QG, 2019. Research on the multi-component gas hydrates: Structure characteristics, formation and dissociation process. Beijing, Chinese Academy of Geological Sciences, PhD thesis, 1–137 (in Chinese with English abstract).

Meng QG, Liu CL, He XL, Ye YG, Zhu YH, Xia N. 2011. Laser-Raman spectroscopy characteristics of natural gas hydrates from Qilian Mountain permafrost. Geological Bulletin of China, 30(12), 1863–1867 (in Chinese with English abstract). doi: 10.3969/j.issn.1671-2552.2011.12.008.

Meng QG, Liu CL, Li CF, Hao XL. 2022. Experimental study on the forming process of multi-component gas hydrates in Qilian Mountain permafrost area. Marine Geology Frontiers, 38(1), 72–79 (in Chinese with English abstract). doi: 10.16028/j.1009-2722.2020.128.

Meng QG, Liu CL, Li CF, He XL, Wang FF, Lu ZQ, Wen HJ, Li YH, Wang WC. 2015. Raman spectroscopic characteristics of natural gas hydrates from Juhugeng drilling area, Qinghai. Geoscience, 29(5), 1180–1188 (in Chinese with English abstract). doi: 10.3969/j.issn.1000-8527.2015.05.022.

Milkov AV. 2004. Global estimates of hydrate-bound gas in marine sediments: how much is really out there? Earth-Science Reviews, 66(3), 183–197. doi: 10.1016/j.earscirev.2003.11.002.

Su K, Zhang GB, Sun YH, Li SL, Guo W. 2016. Formation mechanism and phase state of hydrates in fractured layers of permafrost. Petroleum Drilling Techniques, 44(2), 93–98 (in Chinese with English abstract). doi: 10.11911/syztjs.201602016.

Sun YB, Zhao TH, Cai F. 2013. Gas hydrate resource assessment abroad and its implications. Marine Geology Frontiers, (1), 27–35 (in Chinese with English abstract).

Tian M, 2018. Study on formation and decomposition process of mixed gas hydrate. Qingdao, Qingdao University, Master thesis, 1–52 (in Chinese with English abstract).

Wang F, Li HJ. 2010. Resource assessment methods of gas hydrate accumulations in gulf of Mexico. Marine Geology Letters, 26(3), 59–66 (in Chinese with English abstract). doi: 10.16028/j.1009-2722.2010.03.008.

Wang PK, Zhu YH, Lu ZQ, Bai MG, Huang X, Pang SJ, Zhang S, Liu H, Xiao R. 2019. Research progress of gas hydrates in the Qilian Mountain permafrost, Qinghai, Northwest China: Review. Scientia Sinica Physica, Mechanica and Astronomica, 49(3), 034606 (in Chinese with English abstract). doi: 10.1360/SSPMA2018-00133.

Wang PK, Zhu YH, Lu ZQ, Guo XW, Huang X. 2011. Gas hydrate in the Qilian Mountain permafrost and its distribution characteristics. Geological Bulletin of China, 30(12), 1839–1850 (in Chinese with English abstract). doi: 10.3969/j.issn.1671-2552.2011.12.005.

Ye JL, Qin XW, Xie WW, Lu HL, Ma BJ, Qiu HJ, Liang JQ, Lu JA, Kuang ZG, Lu C, Liang QY, Wei SP, Yu YJ, Liu CS, Li B, Shen KX, Shi HX, Lu QP, Li J, Kou BB, Song G, Li B, Zhang HE, Lu HF, Ma C, Dong YF, Bian H. 2020. The second natural gas hydrate production test in the South China Sea. China Geology, 3(2), 197–209. doi: 10.31035/cg2020043.

Zhang L. 2016. Determination and applications of rock quality designation (RQD). Journal of Rock Mechanics and Geotechnical Engineering, 8(3), 389–397. doi: 10.1016/j.jrmge.2015.11.008.

Zhang W, Li CF, Liu CL, Hu GW, Meng QG, Huang XD, Zhao SJ. 2016. Identification technology of the CT images for distinguishing the boundary condition of methane hydrate in porous media. CT Theory and Applications, 25(1), 13–22 (in Chinese with English abstract). doi: 10.15953/j.1004-4140.2016.25.01.02.

Zhou YW, Guo DX, Qiu GQ, 2000. Permafrost in China. Beijing, Science Press, 329–353. (in Chinese)

Zhu YH, Pang SJ, Xiao R, Zhang S, Lu ZQ. 2021. Natural gas hydrates in the Qinghai-Tibet Plateau: Characteristics, formation, and evolution. China Geology, 4(1), 17–31. doi: 10.31035/cg2021025.

Zhu YH, Zhang YQ, Wen HJ, Lu ZQ, Jia ZY, Li YH, Li QH, Liu CL, Wang PK, Guo XW. 2010. Gas hydrates in the Qilian Mountain permafrost, Qinghai, Northwest China. Acta Geologica Sinica (English Edition), 84(1), 1–10. doi: 10.1111/j.1755-6724.2010.00164.x.